

Parametrized model for obtaining electron scattering rates from radio-frequency size-effect data

J. C. Kimball, Louis W. Adams, Jr., and R. G. Goodrich

Department of Physics and Astronomy, Louisiana State University, Baton, Rouge, Louisiana 70803

(Received 31 October 1978)

A model calculation for the amplitude of radio-frequency size-effect signals as a function of temperature and sample thickness is presented. The model includes impurity scattering, electron-phonon scattering, scattering effectiveness, effective Debye temperature, energy-dependent scattering, and bulk resistance effects. By adjusting the parameters involved in the model to fit experimental data, both the impurity and electron-phonon scattering rates at the Fermi energy are obtained for an orbit on the copper Fermi surface.

I. INTRODUCTION

In an earlier paper¹ we gave a prescription for determining both the electron-phonon ($e-p$) and electron-impurity (ν_i) scattering rates for conduction electrons in metals. These scattering rates were obtained from the radio-frequency size effect² (RFSE) and make use of both temperature- and sample-thickness-dependent data to extract the two scattering rates. The reader is referred to Ref. 1 for a complete description of both the experimental technique and the approximations made in the data-analysis procedure. A brief outline of the previous work and some new observations are given in the next paragraph.

The measured amplitude of a parallel-field RFSE signal from an extremal Fermi surface (FS) orbit is governed by the probability that an electron can traverse the sample without being scattered.² Thus the amplitude A of a parallel-field RFSE signal is given by

$$A = A_0 \sum_{m=1}^{\infty} \exp(-m\pi\bar{\nu}_{\text{eff}}/\Omega) \\ = A_0 [\exp(\pi\bar{\nu}_{\text{eff}}/\Omega) - 1]^{-1}, \quad (1)$$

where $\bar{\nu}_{\text{eff}}$ is the average effective collision frequency for all types of scattering along an orbit, and $\Omega = eH/m^*c$ is the cyclotron frequency, m^* being the cyclotron mass for the orbit and A_0 a constant. We assume here that m^* is the measured enhanced mass which is experimentally obtained. In Ref. 1 it is shown that for a sample of thickness d , if $\ln A$ is plotted against the cube of the absolute temperature T^3 , then the relationship between the slope s of that plot and d is given by

$$\frac{d}{s} = \frac{k_c \hbar}{\pi m^* C} \{1 - \exp[-(\pi m^*/k_c \hbar)\nu_i d]\}. \quad (2)$$

In this expression $k_c = Hed/\hbar c$ is the measured reciprocal-space diameter of the orbit, C is the

$e-p$ scattering frequency per $^{\circ}K^3$, and ν_i is the temperature-independent scattering frequency. This type of analysis was used to extract the values of C and ν_i for an orbit on copper in Ref. 1 and then used extensively for analyzing temperature-dependent RFSE data on silver³ to obtain the anisotropy of the $e-p$ scattering rates. Several problems have arisen in applying the formulation given above to data on other materials and the fit to the data on copper as given in Ref. 1 is not within experimental error in all cases.

The rationale for the present investigation is as follows:

(i) In the previously reported analysis of the copper data the exact expression, Eq. (1), did not agree with experiment for very thin samples. Theory predicts a curvature in the $\ln A$ vs T^3 plot (Fig. 3 of Ref. 1). None was observed experimentally and this has been verified since that time.⁴

(ii) The fit was made to the data assuming the $e-p$ scattering rate was a constant for all electrons participating in the signal. It has been previously shown⁵ that an average $e-p$ scattering rate is measured because an individual electron $e-p$ scattering rate depends on an electron's energy. This is particularly important for data on thick samples where only the longest-lived electrons, i.e., those nearest to the Fermi energy, contribute to a signal.

(iii) In Ref. 1 all phonons were assumed to be effective in removing an electron from the RFSE signal. In reality, small wave vector q phonons will not always remove an electron from an RFSE signal. This fact leads to a correction in the $\ln A$ vs T^3 dependence at low temperatures.

(iv) While it is not a problem in copper or silver, the $e-p$ scattering can become ineffective for phonons with wave vectors larger than the Fermi surface dimensions on which the orbit is being observed. This effect can lead to other than a T^3 dependence of the experimental data as is ob-

served in bismuth⁶ and antimony.⁷

In the analysis procedure that follows, the effects given in (ii)–(iv) above are included and a fourth effect giving rise to an additional T^5 dependence is included. Overall the copper data are fit very well for all sample thicknesses and a more realistic interpretation of the derived parameters is given.

II. SCATTERING MODEL

The purpose of the exercise that follows is to develop a more complete parametrized model with which parallel field RFSE temperature-dependent data can be analyzed. Therefore we give the elements of the model and how they are folded into a data-fitting procedure. The physical quantities obtained from this process and their implications are also discussed. Sections IIA–IIH below describe the elements of our model.

A. Impurity scattering rate

The impurity scattering rate is assumed to be independent of temperature. If ν_I is the impurity scattering rate, then the RFSE signal amplitude is multiplied by $\exp(-\nu_I/\Omega)$ and we set

$$\exp(-\nu_I/\Omega) = Z^d, \quad (3)$$

where Z is treated as an adjustable parameter in the data-fitting process from which ν_I can be obtained. Note that $\Omega \propto H \propto 1/d$ for the RFSE signal.

B. Electron-phonon interaction

The electron-phonon interaction involving the electrons contributing to the signal includes the fact that the scattering rate is dependent on an individual electron's energy ϵ relative to the Fermi energy E_F . As was previously shown by Gantmakher⁸ and Wagner and Albers,⁵ the e - p scattering rate due to the processes shown in Fig. 1 is

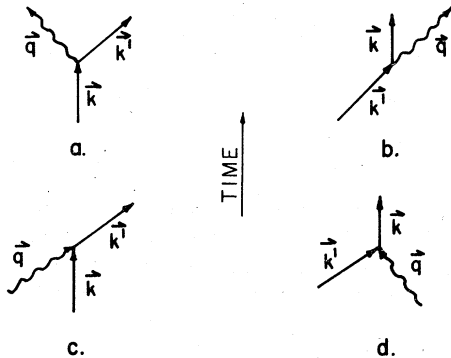


FIG. 1. Diagrams for scattering processes considered in deriving Eq. (4). The vectors \mathbf{k} represent electrons contributing to a signal, thus (a) and (c) represent scattering out of an orbit and (b) and (d) into the orbit.

given by

$$\Gamma(\epsilon, q) = Cq \left(\frac{2}{\exp(\beta \hbar \omega_q) - 1} + \frac{1}{\exp[\beta(\epsilon + \hbar \omega_q)] + 1} + \frac{1}{\exp[\beta(-\epsilon + \hbar \omega_q)] + 1} \right) \delta(\hbar \omega_q - \epsilon - \epsilon'). \quad (4)$$

Here q is the magnitude of the phonon wave vector and $\hbar \omega_q$ is the phonon energy. The overall factor of q arises from an assumption that the squared matrix element for the interaction is proportional to q and the δ function assures energy conservation. The total scattering rate is an average of $\Gamma(\epsilon, q)$ over ϵ and q . The weighting function for the energy average is the derivative of the Fermi function $f'(\epsilon)$ and the average over phonons must be consistent with energy conservation. This leads to the following sequence for the phonon integrals

$$\int d^3q \rightarrow \int_{\text{Fermi surface}} d^3q \cong 2\pi \int_0^{2q_F} q dq. \quad (5)$$

We have implicitly assumed a spherical FS in this approximation. The results are adequate for copper without introducing another adjustable parameter to account for nonspherical FS shapes.

C. Effectiveness function $\gamma(q)$

It has been previously pointed out⁸ that when phonons of wave vector q satisfy the condition

$$q/q_F \ll \delta/d, \quad (6)$$

where δ is the skin depth, d is the sample thickness, and q_F is a phonon of wave vector equal to the Fermi surface radius for the electron being scattered, these phonons will not remove an electron from an RFSE signal. Thus, when averaging the e - p matrix element over q , an effectiveness function $\gamma(q)$ should be included. The appropriate function is derived in the Appendix. The functional form that is derived there is closely approximated by

$$\gamma(q) = \tanh(\omega_q d / \alpha), \quad (7)$$

and we use this form in the data-fitting procedure. The parameter α is adjustable and is used to fit the experimental data.

D. Effectiveness parameter α

Several years ago Gantmakher⁸ pointed out that phonons would be ineffective in scattering electrons when their wave vectors were larger than twice the k -space dimensions of the piece of FS on which an RFSE orbit was observed. This fact has also been discussed in connection with e - p scattering in the electrical resistivity of bismuth⁹

and antimony¹⁰ where the FS dimensions are small compared to phonon wave vector magnitudes. In copper this is not a predominate effect at lower (1–10° K) temperatures, but in order to make the analysis procedure more complete, we allow for this possibility in our overall fitting procedure. The physical fact that e - p scattering has a cutoff when $q \geq 2k_F$ is manifest in the integral of phonons over $\Gamma(\epsilon, q)$ having a noticeable temperature dependence when $2k_F/q \approx 5$ or less. The upper limit of the phonon averaging integral is the ratio of the maximum phonon wave vector q_D to the average q at the temperature of interest. In temperature units the upper limit is Θ_D/T , where Θ_D is the Debye temperature. The effect of the cutoff for small pieces of Fermi surface is to cause the effective Θ_D , Θ_D^* to be much smaller than that corresponding to the maximum phonon energy. A complete discussion of these considerations is given in Ref. 10. We use Θ_D in the upper limit of integration for copper since the cutoff condition $q \geq 2k_F$ is not approached in this case.

The effectiveness parameter α has a simple physical interpretation due to Eq. (6). Rewrite Eq. (6) as

$$qd/q_F \delta = \omega_q d / \omega_{q_F} \delta = \omega_q d / \Theta_D^* \delta > 1. \quad (8)$$

Phonons become effective when

$$\omega_q d / \alpha > 1. \quad (9)$$

Thus, α should be of order $\Theta_D^* \delta$. This shows that if Θ_D^* is low the scattering out of an RFSE orbit becomes effective at lower temperatures than for larger values of Θ_D^* . That is, for small pieces of FS the scattering is effective at lower temperatures than for larger pieces of FS.

E. Effective scattering rate

In order to compare the e - p scattering rate $\Gamma(\epsilon, q)$ with experimental data, an average over phonons that is weighted by the effectiveness function must be taken. Thus,

$$\langle \Gamma(\epsilon) \rangle = \int_0^{q_{\max}} \Gamma(\epsilon, q) \gamma(q) d^3 q. \quad (10)$$

This effective scattering rate can be most easily calculated by making the change of variables $y = \beta \omega_q$ and $x = \beta \epsilon$. Then $\Gamma(\epsilon)$ is proportional to $T^3 H(x)$, given by

$$T^3 H(x) = T^3 \int_0^{\Theta_D^*/T} \tanh\left(\frac{T y d}{\alpha}\right) y^2 \times \left(\frac{2}{e^y - 1} + \frac{1}{e^{x+y} + 1} + \frac{1}{e^{-x+y} + 1} \right) dy. \quad (11)$$

There are two adjustable parameters in our formation so far: Θ_D^* and α . For large values of Θ_D the integral is insensitive to the magnitude of Θ_D^* and Θ_D is a reasonable value to use. When Θ_D^* is of order five times or less the temperature range over which data are obtained, then its precise value becomes an important factor in a data-fitting procedure. The numerical value of α is determined by the lowest temperature data of $\ln A$ vs a function of T .

F. Single-pass formula

In the final averaging process an average of electrons of different energies near the Fermi energy must be performed. The probability that a given electron will traverse a sample of thickness d is given by

$$P = Z^d \exp[-G d T^3 H(x)]. \quad (12)$$

It is P , not $H(x)$, that must be averaged over different electrons. Using the symmetry $H(x) = H(-x)$ and the identity for the derivative of the Fermi function

$$f'(x) = \frac{1}{4 \cosh^2(\frac{1}{2}x)} \quad (13)$$

the integral to be performed is

$$A_1 = \frac{A_0}{2} \int_0^\infty \frac{Z^d \exp[-G d T^3 H(x)]}{\cosh^2(\frac{1}{2}x)} dx.$$

This is the single-pass formula for the RFSE amplitude, where G is the e - p scattering rate per $^\circ\text{K}^3$.

G. Total RFSE amplitude

The quantity A_1 is not the total RFSE amplitude, because it may be possible that electrons will traverse the sample thickness more than once. Define the amplitude for N traverses to be

$$A_N = \frac{A_0}{2} \int_0^\infty \frac{\exp[-G N d T^3 H(x)]}{\cosh^2(\frac{1}{2}x)} Z^{Nd} dx. \quad (14)$$

Then the measured signal amplitude will be

$$A = \sum_{N=1}^\infty A_N. \quad (15)$$

The expression for A_N/A_0 contains four adjustable parameters: G , the electron-phonon scattering strength; α , the effectiveness parameter; Θ_D^* , the effective Debye temperature; and ν_I , the impurity scattering frequency.

H. Correction to multiple-pass expression

In (i) of Sec. I we pointed out that the exact expression for A , Eq. (1), showed curvature when

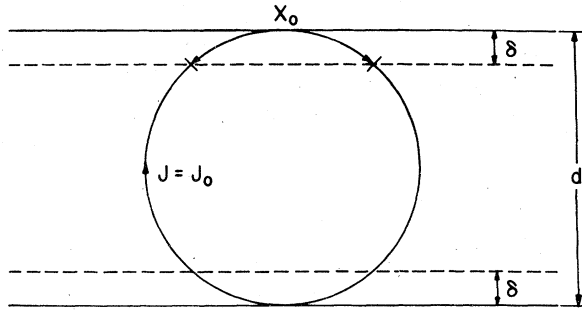


FIG. 2. Current and sample configuration that lead to a T^5 dependence of $\ln A$.

$\ln A$ was plotted against T^3 . So does Eq. (15). This deviation from a T^3 law increases as sample thickness decreases and is only appreciable at the high-temperature end of measurement ranges. Empirically we have found that the addition of a scattering frequency proportional to T^5 and \sqrt{d} gives the required correction to the multiple-pass expression, Eq. (15), and causes the experimentally observed T^3 behavior to be predicted. In what follows we give a simple justification of why this type of behavior might be expected.

In making an RFSE measurement, one in general applies an electric field E_0 in the skin depth of a sample and monitors the changes in E_0 due to the current produced in the skin depth to cancel it. The solution to this problem involves a very complicated surface-impedance calculation that has been worked on by many authors over the past few years. The $\sqrt{d}T^5$ dependence can be roughly obtained by assuming that the induced current in the skin depth satisfies Newton's law with a damping term. That is,

$$\frac{dJ}{dt} = \xi E_0 - \frac{J}{\tau}, \quad (16)$$

where ξ can only be determined from a complete impedance calculation and τ is a relaxation time for the surface current that, because it is a bulk property, is proportional to T^{-5} . During an RFSE resonance the surface currents are altered somewhat, because the orbiting electrons that just span the sample thickness cause a current flow J_0 , whether or not E_0 is present. This current exists over a distance X_0 in the skin depth as shown in Fig. 2. Since the RFSE measurement conditions are such that the rf electric field appears static to the orbiting electrons ($\omega_{rf} \ll \Omega$), the relevant time in which a resonant set of electrons would be involved in the surface current is the time spent in the skin depth. If v is the velocity of electrons on the resonant orbit, then $t = X_0/v$ is the time of importance. The limits of integration for Eq. (16) are $J = J_0$ at $t = 0$ and $J = J(t)$ at $t = t$, and the result

of integration is

$$J(t) = \xi E_0 \tau + (J_0 - \xi E_0 \tau) e^{-t/\tau}. \quad (17)$$

The interesting part of this equation for the RFSE is that part proportional to J_0 , for that is the portion contributing to the RFSE amplitude J_R . Thus, the signal amplitude should in fact be proportional to $J_R = J_0 \exp(-t/\tau)$, where J_0 is proportional to Eq. (15). From Fig. 2 it can be seen that $X_0 \approx 2d\sqrt{\delta/d} \propto \sqrt{d}$. Now, since $1/\tau \propto T^5$ and $t = X_0/v \propto \sqrt{d}$, these considerations predict that $\ln A$ contain an additional term proportional to $T^5\sqrt{d}$. Much more sophisticated considerations are required to obtain the magnitude of this term and we include the magnitude as an adjustable parameter.

This concludes the factors included in our model. All of these factors can be summarized as follows:

$$A = A_0 \sum_{N=1}^{\infty} A_N \exp(-QT^5\sqrt{d}) \quad (18)$$

or

$$\ln(A/A_0) = \ln[\text{Eq. (15)}] - QT^5\sqrt{d}. \quad (19)$$

The final fit to the data then requires five adjustable parameters including Q , only four of which are totally independent [see Eqs. (8) or (9)]. In practice it is possible to either measure or calculate Θ_D^* from other considerations so only four parameters, ν_I , G , α , and Q will in general be determined from fits of this theory to experimental data.

III. COMPARISON TO DATA FROM COPPER

In order to compare the results of this scattering-model calculation to experimental data, we have adjusted the parameters in the model to give a good fit to our previous data from copper. In Fig. 3 the results of a least-squares fit to the temperature-dependent amplitude of RFSE signals for four copper sample thickness are shown as solid lines. No deviation from the T^3 behavior is found in the measurement temperature range. The result of adjusting the parameters of the present model calculation are shown by the dashed lines. Table I gives the values of the slopes of these lines.

In fitting the adjustable parameters to these data the values that were obtained are: $\alpha = 0.8$, $Z = 0.003$, $G = 0.00036$, $Q = 5 \times 10^{-6}$, and $\Theta_D^* = 300$ K. The value of Θ_D^* is not crucial to this fit other than the fact that is much greater than the highest temperature at which measurements were performed. Any value of Θ_D^* greater than 100 K yields the same fit with the same values for the other four parameters. In general, the data fitting procedure involves three operations: (i) the

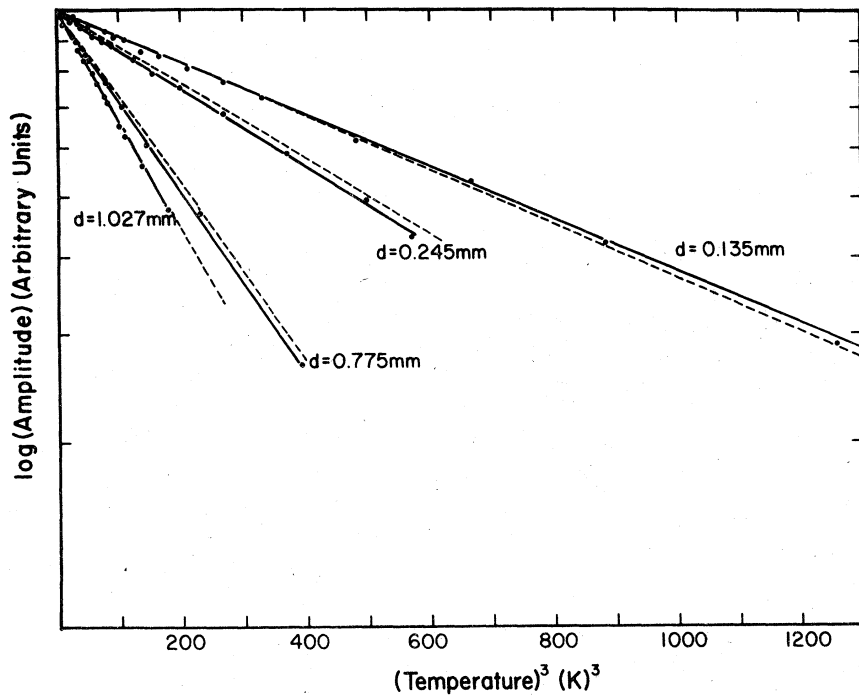


FIG. 3. $\ln A$ vs T^3 for samples of copper all with surface normals parallel to [001] and \vec{H} 15° from [100]. The different curves are explained in the text.

curves must be linear in T^3 for all sample thicknesses, (ii) the change in slope of the lines must agree with the data, and (iii) the magnitudes of the slopes must be correct. The four adjustable parameters contribute to these demands in different ways with only a small amount of parameter interaction.

The value of Q is adjusted to cause the thin samples to exhibit a T^3 behavior at high temperatures and it has very little effect on thick samples. The parameter P is mainly important in causing the low-temperature results to obey a T^3 dependence. The value of G strongly affects the overall magnitude of the slopes and Z is adjusted to yield the correct differences in slopes from one sample thickness to the next.

Values of $\bar{\nu}_I$ and $\bar{\nu}_P/T^3$ for this orbit can be calculated respectively from the values of Z and G given above. They are

$$\bar{\nu}_I = 4.3 \times 10^9/\text{sec}, \quad \bar{\nu}_P/T^3 = 2.24 \times 10^6/\text{sec K}^3.$$

The corresponding values of Johnson *et al.*¹ are $\bar{\nu}_I = 3.7 \times 10^9/\text{sec}$ and $\bar{\nu}_P/T^3 = 3.7 \times 10^6/\text{sec K}^3$. The difference between the current value of $\bar{\nu}_I$ and that obtained by Johnson *et al.*,¹ is only 15% which is within experimental error. However, the value of $\bar{\nu}_P/T^3$ obtained here is much smaller than any previous measurement for this orbit, the difference being of order 35%. This is because in previous analyses of experimental data it was assumed that $\bar{\nu}_P/T^3$ was energy independent. This is not the case and the theory used to analyze previous data is incorrect in that a constant scattering rate, independent of electron energies has been applied to all previous results. What one obtains experimentally is an average (over electron energy) scattering rate whereas the value of $\bar{\nu}_P/T^3$ given above is the value at the Fermi energy. This analysis does not disagree with previous work, but points out that

$$\left. \frac{\bar{\nu}_P}{T^3} \right|_{E_F} < \left. \frac{\bar{\nu}_P}{T^3} \right|_{\text{energy average}}$$

TABLE I. Sample thickness d and corresponding values of the slopes of $\ln A$ vs T^3 plots for both the experimental data and the model calculation.

| d (mm) | Experimental slope ($^\circ\text{K}^{-3}$) | Calculated slope ($^\circ\text{K}^{-3}$) |
|----------|--|--|
| 1.027 | 4.19×10^{-3} | 4.34×10^{-3} |
| 0.775 | 3.34×10^{-3} | 3.31×10^{-3} |
| 0.245 | 1.48×10^{-3} | 1.39×10^{-3} |
| 0.135 | 1.02×10^{-3} | 1.01×10^{-3} |

The fact that the electron-phonon scattering rate exhibits a strong energy dependence has been discussed in detail by Wagner and Albers.⁵

ACKNOWLEDGMENT

This work was supported in part by the NSF under Grant No. DMR76-81866.

APPENDIX

In this Appendix a model calculation for $\gamma(q)$, the probability that a phonon of momentum q scatters an electron out of an RFSE orbit is given.

We presume the sample is homogeneous and isotropic with smooth parallel faces separated by a distance d . The ratio-frequency electric field penetrates both surfaces a skin depth δ where $\delta \ll d$. Additionally we assume the radius of the electronic orbits (recall the external magnetic field is parallel to the sample surfaces) most effective in the resonance process to be

$$r = \frac{1}{2}(d - \delta).$$

Let Δ represent a spatial translation of the circular resonance orbit in a direction perpendicular to the sample surfaces. It can be shown that a spatial translation Δ leads to new trajectory intersecting a surface of the sample with probability

$$P(\Delta) = \begin{cases} \Delta/\delta & \text{if } \Delta < \delta \\ 1 & \text{if } \Delta > \delta. \end{cases}$$

Kinematic considerations for the electron-phonon scattering will determine how the spatial translation occurring as a consequence of such an event is a function of the initial electron momentum \vec{k} and the phonon momentum \vec{q} . Here $q \ll k$ and only the direction of the electron momentum is significantly altered by the phonon absorption or emission as described below.

If one assumes that the Fermi surface of the material is spherical, then the initial and final electron momenta, \vec{k} and \vec{k}' , respectively, will be of essentially equal magnitude. Furthermore, \vec{k} and \vec{q} will essentially be at right angles. Because of this only phonons approaching or leaving the electron in a plane perpendicular to \vec{k} may scatter the electron; other phonons would violate the energy conservation requirement.

The electron momentum is always perpendicular to the radius vector of the circular resonance orbit and in this way, given r , the direction of the electron momentum defines the center of the orbit. Phonon absorption or emission yields a new direction for the electron momentum and a new orbit center is consequently established. For an illustration of this point and as a guide to what

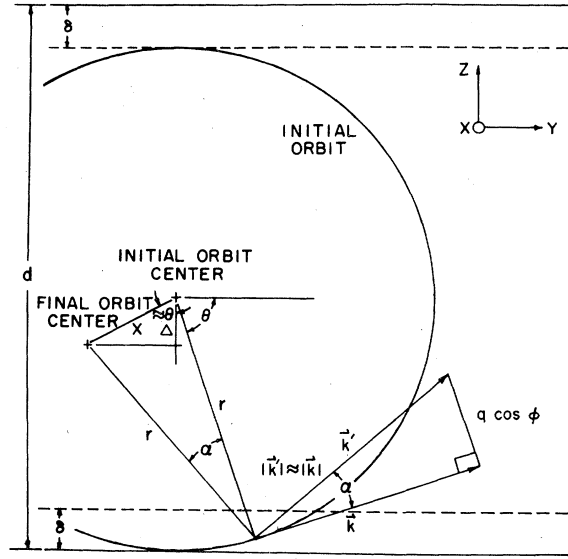


FIG. 4. Geometry necessary for the scattering effectiveness calculation.

follows see Fig. 4. A new orbit corresponds to a translation Δ of the orbit towards or away from a sample surface. The direction of \vec{q} will be parametrized by two angles θ and ϕ in a way that conforms to our remarks in the previous paragraph. Our subsequent derivation ignores the role of the x component of \vec{q} in the scattering from resonance. We expect this to be non-negligible only for large q .

All of the preceding assumptions are incorporated into the diagram shown in Fig. 4 and from this it is seen that

$$\Delta \approx x |\cos \theta| \approx \frac{r q}{k} |\cos \phi \cos \theta| = \frac{q \delta}{q_{\text{crit}}} |\cos \phi \cos \theta|,$$

where a critical phonon momentum

$$q_{\text{crit}} = 2k\delta/d$$

has been introduced. In terms of these parameters the probability of an orbit intersecting a surface becomes

$$P(\vec{q}) = \begin{cases} \frac{q}{q_{\text{crit}}} |\cos \phi \cos \theta|, & \text{if } \frac{q \delta}{q_{\text{crit}}} |\cos \phi \cos \theta| < 1 \\ 1, & \text{if } \frac{q \delta}{q_{\text{crit}}} |\cos \phi \cos \theta| > 1. \end{cases}$$

The total scattering probability is obtained by integration over the orbit as follows:

$$\gamma(q) = \int_0^{2\pi} \int_0^{2\pi} P(\vec{q}) d\phi d\theta / \int_0^{2\pi} \int_0^{2\pi} d\phi d\theta.$$

This integration, in general, must be done numerically because the analytic form for $P(\vec{q})$ depends on an inequality involving q , ϕ , and θ .

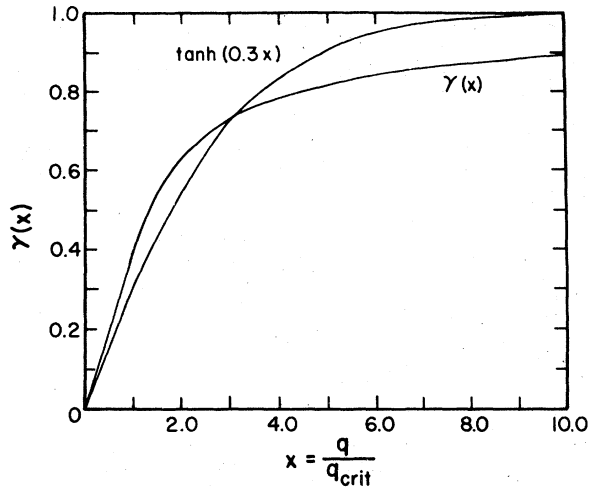


FIG. 5. Results of numerical integration for $\gamma(q)$ and the approximate function used for $\gamma(q)$ in the fitting procedure.

However, in the case where $q \leq q_{\text{crit}}$, the integration can be done analytically and we find

$$\gamma(q) = \frac{4}{\pi^2} \frac{q}{q_{\text{crit}}} \quad \text{for } q \leq q_{\text{crit}}.$$

The result of numerical integration for $\gamma(q)$ out to $q/q_{\text{crit}} = 10.0$ is shown in Fig. 5. In addition a plot of the hyperbolic tangent of $0.3x$ is given to show its similarity to $\gamma(q)$ and justify its use in our numerical fitting procedure. An approximation used in obtaining $\gamma(q)$ causes the curve to underestimate the scattering probability at large values of q . This is because the x component of \vec{q} for large $|\vec{q}|$ will become effective in scattering electrons from resonance. Since this mechanism was not included in the model, the hyperbolic tangent function used to represent $\gamma(q)$ in the fitting procedure is justifiable because it gives slightly larger values of the scattering probability than does $\gamma(q)$ at large q but has qualitatively the same shape.

¹P. B. Johnson, J. C. Kimball, and R. G. Goodrich, Phys. Rev. B **14**, 3282 (1976).

²For a review of the RFSE see V. F. Gantmakher, Prog. Low Temp. Phys. **5**, 181 (1967).

³P. B. Johnson and R. G. Goodrich, Phys. Rev. B **14**, 3286 (1976).

⁴V. A. Gasparov and N. H. Harutunian, Solid State Commun. **19**, 189 (1976).

⁵D. K. Wagner and R. C. Albers, J. Low Temp. Phys. **20**, 593 (1975).

⁶V. F. Gantmakher and Ju. S. Leonov, Sov. Phys.-JETP Lett. **16**, 180 (1972).

⁷V. F. Gantmakher and V. T. Dolgoplov, Sov. Phys.-JETP **33**, 1215 (1971).

⁸V. F. Gantmakher, Rep. Prog. Phys. **37**, 317 (1974).

⁹C. Uher and W. P. Pratt, Jr., Phys. Rev. Lett. **39**, 491 (1977).

¹⁰C. L. Tsai, D. Waldorf, K. Tanaka, and C. G. Grenier, Phys. Rev. B **17**, 618 (1978).